0026-895X/06/7005-1621–1629$20.00
MOLECULAR PHARMACOLOGY
Copyright © 2006 The American Society for Pharmacology and Experimental Therapeutics
Mol Pharmacol 70:1621–1629, 2006

Vol. 70, No. 5
24273/3151181
Printed in U.S.A.

A Single Decoy Oligodeoxynucleotides Targeting Multiple Oncoproteins Produces Strong Anticancer Effects

Huanhuan Gao, Jiening Xiao, Qiang Sun, Huixian Lin, Yunlong Bai, Long Yang, Baofeng Yang, Huizhen Wang, and Zhiguo Wang

Research Center, Montreal Heart Institute, Montreal, Quebec, Canada (H.G., J.X., Q.S., H.L., L.Y., H.W., Z.W.); Department of Medicine, University of Montreal, Montreal, Quebec, Canada (Z.W.); and Department of Pharmacology (State-Province Key Lab of China) (Y.B., B.Y.) and Institute of Cardiovascular Research (J.X., H.L., B.Y., Z.W.), Harbin Medical University, Harbin, People's Republic of China

Received March 8, 2006; accepted August 25, 2006

ABSTRACT

Cancer in general is a multifactorial process. Targeting a single factor may not be optimal in therapy, because single agents are limited by incomplete efficacy and dose-limiting adverse effects. Combination pharmacotherapy or "drug cocktail" therapy has value against many diseases, including cancers. We report an innovative decoy oligodeoxynucleotide (dODN) technology that we term complex decoy oligodeoxynucleotide (cdODNs) in which multiple *cis* elements are engineered into single dODNs attacking multiple target transcription factors, mimicking the drug cocktail approach. We designed dODNs targeting NF-κB, E2F, and Stat3 separately and a cdODN targeting NF-κB, E2F, and Stat3 concomitantly. We evaluated effects of this cdODN on expression of cancer-related genes, viability of human cancer cell lines, and in vivo tumor growth in nude mice. The cdODN targeting all NF-κB, E2F, and Stat3 together demonstrated enhancement of efficacy of more than 2-fold and increases in potency of 2 orders of magnitude compared with each of the dODNs or the combination of all three dODNs. The cdODN also showed earlier onset and longer-lasting action. Most strikingly, the cdODN acquired the ability to attack multiple molecules critical to cancer progression via multiple mechanisms, leading to elimination of regression. Real-time reverse transcription-polymerase chain reaction revealed that the cdODNs knocked down expression of the genes regulated by the target transcription factors. The cdODN strategy offers resourceful combinations of varying *cis* elements for concomitantly targeting multiple molecules in cancer biological processes and opens the door to "one-drug, multiple-target" therapy for a broad range of human cancers.

Cancers, like most other human diseases, are multifactorial and multistep processes, progressing by the accumulation of genetic abnormalities in somatic cells, allowing them to escape from control mechanisms involved in cell differentiation, growth, and death. Targeting a single factor (molecule) may not be adequate and certainly not optimal in cancer therapy, because single agents are limited by incomplete efficacy and dose-limiting adverse effects. If related factors are concomitantly attacked, better outcomes are expected, and the current combination pharmacotherapy was developed for this reason: a combination of two or more drugs or therapeutic agents given as a single treatment that successfully saves lives. The "drug cocktail" therapy of AIDS is one example of such a strategy (Henkel, 1999), and similar approaches have been used for a variety of other diseases, including cancers (Konlee, 1998; Charpentier, 2002; Ogihara, 2003; Kumar, 2005; Lin et al., 2005a; Nabholtz and Gligorov, 2005). However, the current drug-cocktail therapy is costly and may involve complicated treatment regimen, undesired drug-drug interactions, and increased side effects (Konlee, 1998). There is a need to develop a strategy to avoid these problems, and a "one-drug, multiple-target" strategy is highly desirable. However, it is nearly impossible to confer to single compounds the ability to act on multiple target molecules with the traditional pharmaceutical approaches or the currently known antigene strategies.

The decoy oligodeoxynucleotide (dODN) technology in-

This work was supported in part by the Fonds de la Recherche de l'Institut de Cardiologie de Montreal (to Z.W.).
Article, publication date, and citation information can be found at http://molpharm.aspetjournals.org.
doi:10.1124/mol.106.024273.

ABBREVIATIONS: dODN, decoy oligodeoxynucleotide; ODN, oligodeoxynucleotide; TF, transcription factor; sdODN, simplex decoy ODN (a decoy ODN containing only one *cis* element); cdODN, complex decoy ODN (a decoy ODN containing multiple *cis* elements); RT, room temperature; EMSA, electrophoretic mobility shift assay; PBS, phosphate-buffered saline; SSC, standard saline citrate; PI, propidium iodide; FITC, fluorescein isothiocyanate; NES, cdODN with three *cis* elements NF-κB, E2F, and Stat3; N+E+S, coapplication of NF-κB$_1$, E2F$_1$, and Stat3$_1$; NC, negative control; NF-κB, nuclear factor κB.

volves synthetic double-stranded ODN containing a *cis* element with high affinity for a target transcription factor (TF) but with low affinity for nontarget TFs, which can bind the TF after being introduced into target cells and attenuate authentic *cis-trans* interaction, leading to removal of *trans* factors from the endogenous *cis* element with subsequent modulation of gene expression (Bielinska et al., 1990; Morishita et al., 1995, 1997). TFs are known to bind to *cis* elements in a cooperative manner, where one molecule of TF binds weakly but multiple molecules of the same TF engage in protein-protein interactions that increase each of their bindings to the *cis* element. To facilitate TF binding to a dODN, one can elevate molar concentration of dODNs, but this may well elicit toxicity. Otherwise, one can engineer multiple consensus sites into one dODN so that one molecule of dODN could provide a number of binding sites for the target TF, even at lower concentrations. For the sake of clarity, we call the originally defined dODN *simplex decoy ODN* (sdODN), because it generally contains only one binding site for a TF, and we call the dODN incorporating multiple binding sites for multiple TFs *complex decoy ODN* (cdODN). In this study, we compared the effects on tumor cell growth and expression of cancer-related genes of sdODNs targeting NF-κB, E2F, or Stat3 separately and a cdODN targeting the three oncoproteins simultaneously, and we demonstrated the superiority of the latter over the former.

Materials and Methods

Preparation of Decoy ODNs. Single-stranded phosphorothioate oligodeoxynucleotides were synthesized by Integrated DNA Technologies, Inc. (Coralville, IA). The ODNs were washed in 70% ethanol, dried, and dissolved in sterilized Tris-EDTA buffer (10 mM Tris and 1 mM EDTA). The supernatant was purified using Micro Bio-Spin 30 columns (Bio-Rad Laboratories, Hercules, CA) and quantified by spectrophotometry. The double-stranded dODNs were then prepared by annealing complementary single-stranded oligodeoxynucleotides (Fig. 1) by heating to 95°C for 10 min followed by cooling to room temperature (RT) slowly over 2 h.

Cell Culture. Human breast cancer cell lines SKBr-3 and MCF-7 were grown in McCoy's 5a medium, and A549 human lung cancer cells were grown in the Ham's F12K medium (Wang et al., 2002). All the cells and media were purchased from American Type Culture Collection (Manassas, VA).

Electrophoretic Mobility Shift Assay. The dODNs were labeled by mixing 4 μl (50 ng) of annealed dODNs with 4 μl of T4 kinase buffer (5×), 1 μl dithiothreitol (0.1 M), 6 μl of [γ-^{32}P]ATP, 3 μl of double-distilled H_2O, and 2 μl of T4 kinase. The sample was incubated at 37°C for 1 h and then 80 μl of 10 mM Tris-HCL, pH 8.0, was added to complete the reaction. The sample was then loaded into the G-25 column and centrifuged at 7000*g* for 2 min. The nuclear extract of human cancer cell lines SKBr-3 was purchased from Santa Cruz Biotechnology (Santa Cruz, CA). Binding reactions were carried out at RT for 15 min in a buffer containing 1.2 μg of nuclear extracts in 10 μl of H_2O and 8 μl of master mix (12×) containing 1 M Tris-HCl, pH 7.5, 0.5 M EDTA, 5 M NaCl, 1 M dithiothreitol, 50% glycerol, 100 μg/μl bovine serum albumin, and 1 μg/μl poly(dIdC). For supershift experiments, antibodies [1 μg; anti-NF-κB/p65 antibody (Santa Cruz Biotechnology) and anti-E2F and STAT3 (Cell Signaling Technology Inc., Danvers, MA) were included in the reaction. For competition experiments, unlabeled dODNs in 100-fold excess of the labeled dODNs were added in the binding reactions. Then, 2 μl (100,000 cpm/μl)of ^{32}P-labeled dODNs were added to the reaction and incubated for another 15 min at RT, followed by addi-

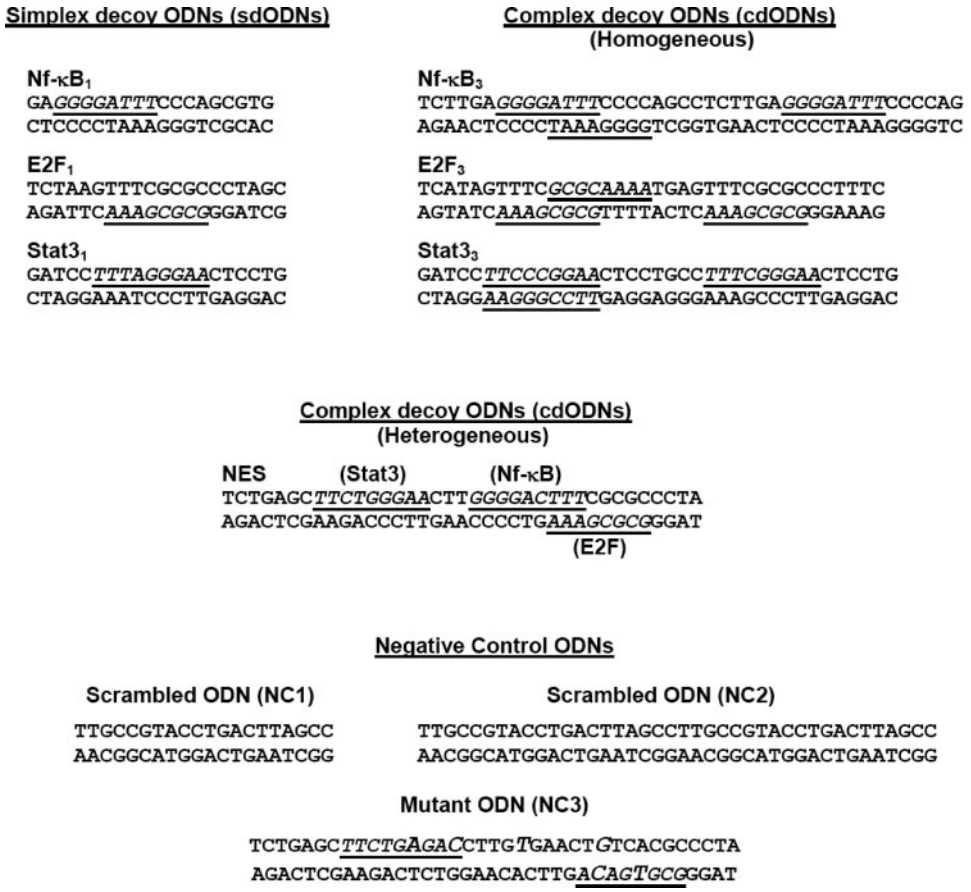

Fig. 1. The dODN sequences designed to specifically target the TFs as specified. The consensus binding sites are italic and underlined, and the number of consensus binding sites for the specified TF is indicated by the value within the brackets attached to the name of TFs. The enlarged letters indicate the substituted nucleotides. For convenience, we labeled the negative control ODNs NC1, NC2 and NC3.

tion of 2 μl of loading dye. DNA-protein complexes were separated by nondenaturing polyacrylamide gel (7.5% in 0.4 × Tris-borate/EDTA) electrophoresis. Gels were dried and analyzed with the Typhoon image system and quantified with ImageQuant software (version 5.2) (GE Healthcare, Little Chalfont, Buckinghamshire, UK).

Decoy ODN Transfection. The cells were transfected with different concentrations of dODNs using Lipofectamine 2000 (Invitrogen, Carlsbad, CA). For viability study, cells were seeded in 96-well tissue culture plates. At 50% confluence, the cells were washed with serum-free medium once and then incubated with 50 μl of fresh fetal bovine serum-free medium. Decoy ODNs of varying concentrations and Lipofectamine (0.25 μl) were separately mixed with 25 μl of Opti-MEM I reduced serum medium (Invitrogen, Carlsbad, CA) for 5 min. Then, the two mixtures were combined and incubated for 20 min at RT. The lipofectamine-dODNs mixture was added dropwise to the cells and incubated at 37°C for 5 h. Thereafter, 25 μl of fresh medium containing 30% fetal bovine serum was added to the well, and the cells were maintained in the culture until use, either for cell growth assays or for RNA extraction.

Subcellular Localization of Transfected dODNs. The dODNs were labeled with Alexa Fluor 488 using *ULYSIS* Nucleic Acid Labeling kits (Invitrogen). The labeled dODNs were purified with Micro Bio-Spin 30 columns (Bio-Rad Laboratories). The cells grown on sterile coverslips in 12-well plates were transfected with the dODNs. At the selected time points after transfection, the cells were washed twice with phosphate-buffered saline (PBS) and fixed with 2% paraformaldehyde for 20 min. To visualize nuclear DNA, the fixed cells were equilibrated in 2× SSC solution (0.3 M NaCl and 0.03 M sodium citrate, pH 7.0) and incubated with 100 μg/ml DNase-free RNase in 2× SSC for 20 min at 37°C. The sample was rinsed three times in 2× SSC and incubated with 5 μM propidium iodide (PI; Invitrogen) for 30 min at RT. The coverslips were mounted onto slides with DABCO medium. The samples were examined under a laser scanning confocal microscope (Zeiss LSM 510) with Alexa Fluor 488 (excitation at 492 nm and emission at 520 nm) or with PI (excitation at 535 nm and emission at 617 nm). The images were analyzed by Zeiss LSM software suite.

Real-Time RT-PCR. RNA was isolated with RNeasy Mini Kit (QIAGEN, Valencia, CA), according to the manufacturer's protocols and treated with DNase I to remove genomic DNA. TaqMan quantitative assay of transcripts was performed with real-time two-step reverse transcription PCR (GeneAmp 5700; Applied Biosystems, Foster City, CA), involving an initial reverse transcription with random primers, as described previously (Pang et al., 2003). Human glyceraldehyde-3-phosphate dehydrogenase control reagents (Applied Biosystems) were used as internal controls.

Determination of Cell Viability. Cell viability was determined by three methods, as described previously in detail (Wang et al., 2002; Ji et al., 2004; Lin et al., 2005a). In the first method, cells were seeded in 96-well tissue culture plates. At 50% confluence, the growth of cells was synchronized in defined serum-free medium for 5 h. The cells were then transfected with decoy ODNs as described above. Sixteen hours later, the cells were washed with PBS, harvested by trypsinization, and suspended in 100 μl of medium. A 10-μl cell suspension was used for manual counting using hemacytometer (Sigma-Aldrich, Horsham, PA), and the counting for each sample was performed in duplicate.

In the second method, cell proliferation was assessed by characterizing the log phase growth with population doubling time (PDT) calculated by using the equation: $1/(3.32 \times (\log N_H - \log N_I)/(t_2 - t_1)$, where N_H is the number of cells harvested at the end of the growth period (t_2) and N_I is the number of cells at 5 h (t_1) after seeding (Wang et al., 2002).

The third method used to determine cell viability in our study was the WST-1 kit (Roche, Penzberg, Germany). In brief, 18 h after treatment with dODNs, cells were washed with PBS and grown in 100 μl of fresh culture medium plus 10 μl of WST-1 reagent for 30 min. The absorbance was measured at 425 nm using a Spectra Rainbow microplate reader (Tecan, Grödig, Austria) with a reference wavelength of 690 nm.

Subcutaneous Tumor Xenografts and Assessment of Growth. The procedures were similar to those described previously (Ji et al., 2004). Four-week-old female BALBc nu/nu nude mice (Charles River Laboratories, Wilmington, MA) were housed five per cage in a pathogen-free environment under controlled conditions of light and humidity in the Animal House of Harbin Medical University on a standard sterilizable laboratory diet. Mice were quarantined for 1 week before experimental manipulation; at the end of the quarantine, SKBr-3 cells (5×10^6) were inoculated s.c. to the left dorsal flank of mice. When tumor size reached ~50 mm (approximately 7 days after inoculation), animals were randomly divided into five groups and NF-κB_1, E2F_1, Stat3_1, the scrambled ODN, NES, or a mixture of all three sdODNs was administered daily by a single intratumoral injection (20 μl of 100 nM dODNs mixed with Lipofectamine 2000). Tumor growth was monitored regularly, and the volume (V) of tumors at day 7 after dODN treatment was calculated using the formula $V = 1/2 \times \text{length} \times (\text{width})^2$. All operative procedures and animal care strictly conformed to Guidelines set by the Animal Ethics Committee of the Harbin Medical University.

Measurement of Uptake of Fluorescent dODNs. One day before treatment, SKBr-3 cells were plated in 24-well format with 1×10^5 cells/well in 500 μl. On the day of treatment, the cells were incubated with FITC-labeled phosphorothioate ODNs (100 nM and 1 μM) in the presence of Lipofectamine 2000 for 4 h. After incubation, the cells were harvested with PBS-EDTA and washed twice with PBS, and then soaked in TBS + 50 mM glycine (10 min). The amount of internalized phosphorothioate ODNs was determined by flow cytometry. The concentration of ODNs associated with SKBr-3 cells was estimated by interpolation from a standard curve of known FITC (Invitrogen).

For measurement of intracellular cdODN concentration in tumor cells from the nude mice, xenograft pieces were dissected from the animals injected with NES (100 nM)-Lipofectamine mix for 3 days and 7 days. The preparation was minced and then digested with 0.5 mg/ml collagenase type IV (Sigma Chemical Co.) at 37°C. Cells were dispersed by trituration and washed three times with PBS. The amount of cell-associated phosphorothioate ODNs was determined by flow cytometry, as described above.

Control Experiments. For all experiments, negative control (NC) was performed with NC1, NC2 or NC3 ODNs (Fig. 1). In particular, for experiments involving sdODNs, NC1 was used; for those with cdODNs, NC2 was used. Additional control was carried out with NC3 as specified. The data presented were all normalized to their respective NCs.

Statistical Analysis. Group data are expressed as mean ± S.E. Statistical comparisons (performed using ANOVA followed by Dunnett's method) were carried out using Microsoft Excel. A two-tailed $p < 0.05$ was taken to indicate a statistically significant difference. Nonlinear least squares curve fitting was performed with Prism software (GraphPad Software, San Diego, CA).

Results

Design of the cdODN. We designed a series of dODNs with consensus sequences for NF-κB, E2F, and Stat3 (Fig. 1) and evaluated the effects of these dODNs on gene transcription, tumor cell growth, and in vivo tumor growth. For convenience, we labeled the sdODNs containing only one *cis* element NF-κB_1, E2F_1, and Stat3_1 and the cdODNs containing three identical *cis* elements NF-κB_3, E2F_3, and Stat3_3. We also integrated the *cis* elements for NF-κB, E2F, and Stat3 together into one cdODN molecule that we designated NES. The criteria for selecting these oncoproteins for targeting were 2-fold. First, these TFs play critical roles in cancer generation and progression and the feasibility of dODNs

targeting these TFs as therapeutic agents for human cancers has been documented (Mann et al., 1999; Ahn et al., 2003; Chan et al., 2004; Leong et al., 2004; Dolcet et al., 2005; Xi et al., 2005; Yokoyama et al., 2005). Use of these TFs should facilitate the comparison between the sdODNs and cdODN. Second, more importantly, we aimed to attack concomitantly multiple processes determining tumorigenesis and cancer progression. NF-κB is known to antagonize apoptosis and promote cell proliferation, E2F is the major factor for the regulation of cell cycle progression, and cumulative evidence supports a role for aberrant Stat3 activation in transformation and tumor progression, partly because of its antiapoptotic effects via repression of p53. By removing the *trans* actions of these TF oncoproteins, one would expect to produce a strong antiproliferation and proapoptotic (and, therefore, anticancer) profile.

The rules for designing cdODNs were set to ensure high affinity, high specificity, and short length principles. First, each of the *cis* elements contained 100% homology to the consensus core sequences for the target TFs and optimal matrix similarity. Second, multiple *cis* elements were organized in a way that should produce the least nonspecific binding to nontargeted TFs; this is one reason that the E2F *cis* element was placed to the antisense strand of the cdODN (NES; Fig. 1). And third, the length of cdODNs was limited to as short as possible without affecting TF binding because short ODNs might be easier to enter into the cell and nucleus and should have less chance to allow for binding by nontarget TFs. This is another reason why, in NES design, the *cis* elements were arranged into both the sense and antisense strands of our NES cdODN. We used the Genomatix (http://www.genomatix.de) to predict the specificities toward their respective TFs to obtain optimal organization and length of multiple *cis* elements in one cdODN. Their ability to bind with the target TFs was examined by EMSA, as described in a later section. Scrambled and mutated dODNs were also designed for negative control experiments (Fig. 1).

Concentration-Dependence of Antigrowth Effects. To examine the above notion, we evaluated the effects of the cdODNs on viability of SKBr-3 human breast cancer cells, compared with those of the sdODNs (Fig. 2), because SKBr-3 cells have been shown to express the target oncoproteins (Li et al., 2004; Lun et al., 2005). The dODNs produced concentration-dependent abrogation of cell numbers, as determined 18 h after transfection of dODNs (see *Time-Dependence of Antigrowth Effects*). Both the homomeric (carrying multiple identical *cis* elements) and heteromeric (carrying multiple distinct *cis* elements) cdODNs demonstrated remarkably greater efficacies and potencies of actions in suppressing cell growth. These were reflected by the downward shifts of dose-response curves with cdODNs relative to with sdODNs. In particular, the cdDNAs had nearly a 2-fold greater maximum effect than the sdDNAs, and even greater intensification (3-fold) was found with NES. The negative controls with scrambled ODNs (NC1 and NC2) did not produced any changes, but NC3 (the mutated NES with nucleotides substitutions) elicited slight depression of cell growth ($p > 0.05$).

The IC_{50} was reduced by 1 order of magnitude with the homomeric cdODNs compared with their relative sdODNs, and NES further reduced the IC_{50} value by another order of magnitude to the picomolar concentration range (Fig. 2). This is particularly important because the scrambled ODN for negative control (both NC1 and NC2, Fig. 1) also demonstrated non-negligible but not statistically significant decreases in gene expression (10%) and cell viability (15%) at 1 μM, suggesting nonspecific and toxic actions of the dODNs at higher concentrations. And by reducing the IC_{50} from 10 to 30 nM with the sdODNs close to the potential toxic concentrations down to 0.8 nM with NES, ~1000-fold lower than the line, the heterogeneous cdODN should have substantially smaller toxicity.

Time-Dependence of Antigrowth Effects. In addition to concentration-dependence, the advantages of cdODNs over sdODNs were also revealed by the time-dependence of the

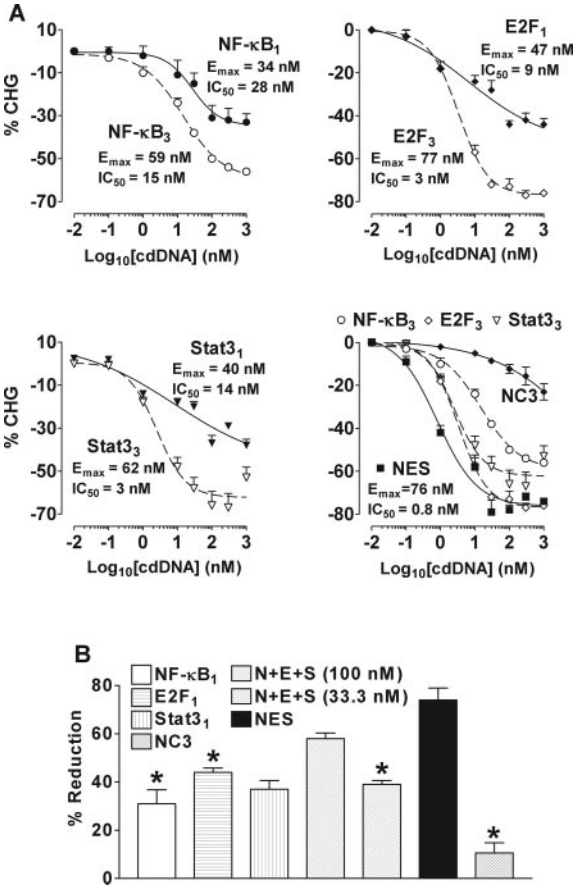

Fig. 2. Validation of the cdODN technology as an anticancer therapeutic approach in an in vitro model using human breast cancer cell line SKBr-3. A, concentration-dependent reduction of cell viability produced by the dODNs: comparisons among the sdODNs, their respective homomeric cdODNs and heteromeric cdODN (NES). Note the downward and leftward shifts of the dose-response curves by cdODNs, relative to the sdODNs, indicating increased maximum effects (E_{max}) and decreased IC_{50}. Symbols are the averaged experimental data, and lines represent the fit to the Hill equation. The mean E_{max} and IC_{50} values ($n = 6$ independent experiments for each group) are indicated, and the values were statistically significant between all cdODNs and sdODNs. The IC_{50} of NES was significantly smaller than all homogeneous cdODNs. All data points reflect normalization with their negative controls (NCs) (i.e., sdODNs normalized to NC1 and cdODNs normalized to NC2). For additional control, NC3 was also normalized to NC2. NC1 and NC2 are scrambled ODNs, and NC3 is a mutated NES with nucleotide substitution in the core sequences of the *cis* elements (see Fig. 1). B, comparison of decreases in cell viability produced by NES and cotransfection of the three sdODNs (N+E+S) as a combination treatment. "N+E+S (100 nM)" indicates a concentration of 100 nM for each sdODN and 300 nM for the total, and "N+E+S (33.3 nM)" indicates a concentration of 33.3 nM for each sdODN and 100 nM for the total. *, $p < 0.05$ versus NES; $n = 6$ independent experiments for each group.

effects (Fig. 3). First, the onset of effects with the cdODNs was much earlier than with the sdODNs; significant diminishment of cell viability took place with cdODNs at approximately 8 h after transfection, well ahead of that with sdODNs, which occurred 12 h after transfection. The effects of sdODNs were biphasic, showing initial time-dependent diminishment of cell viability within 18 h and subsequent time-dependent revitalization up to 72 h after transfection. By comparison, the effects of the homogeneous cdODNs reached the maximum or steady-state levels within 10 h. In sharp contrast, the reduction of cell viability in the cells treated with NES developed continuously over 72 h and became virtually nonrevivable, leading to complete elimination of the cancer cells. These results indicate that simultaneously attacking multiple targets (NF-κB, E2F, *and* Stat3) remarkably enhances anticancer effects compared with attacking only one target (NF-κB, E2F, *or* Stat3). This point was further evidenced by the fact that effects produced by combination treatment via cotransfection of NF-κB_1, $E2F_1$, and $Stat3_1$ (100 nM for each) were somewhat smaller than those by NES (100 nM) (Fig. 2B). It must be noted that the total concentration of the combination treatment was 300 nM, 3-fold higher than NES, further suggesting the superiority of cdODNs over sdODNs. Improved effects with cdODNs are presumably a result of increased affinity of binding to TFs and enhanced stability of protein-protein interactions (and therefore DNA-protein interactions) and of increased target versatility. The data presented above are from manual counting of the viable cells, and the results were confirmed by modified 3-(4,5-dimethylthiazol-2-yl)-2,5-diphenyltetrazolium and flow cytometry methods (data not shown). All these results were consistently reproduced in two other cancer cell lines: A549 human lung cancer cells and MCF-7 human breast cancer cells (data not shown).

In Vivo Antitumor Effects. To further validate our technology, we tested the effectiveness of the cdODNs in inhibiting in vivo tumor growth in nude mice. The mice began to receive daily intratumoral injection of Lipofectamine 2000-treated ODNs from 7 days after subcutaneous inoculation of SKBr-3 cells, and the volume of tumors were measured at fixed time points up to 7 days after drug administration. As depicted in Fig. 4A, the growth of tumors was retarded with the sdODN NF-κB_1, $E2F_1$, or $Stat3_1$ alone, relative to administration of a scrambled control ODN (NC2). With combination therapy (coinjection of all three different sdODNs), the tumors failed to grow and seemed to stabilize. Most strikingly, application of NES resulted in destruction of the tumors, shrinking the tumor mass to a smaller size than before drug treatment. Figure 4B demonstrates that the inhibitory effects on tumor growth were clearly in the order of NES > cotransfection (N+E+S) ≫ NF-κB_1, $E2F_1$, or $Stat3_1$ alone. For instance, NES caused ~78% diminishment of tumor volumes, compared with ~35% and ~63% decreases produced by $E2F_1$ and N+E+S, respectively.

Potential Mechanisms Underlying the Antitumor Effects of cdODNs. To investigate whether the efficacy of the dONDs is attributable to TF "decoy" effects but not to nonspecific cytotoxicity, the following steps were taken. We first verified the ability of the dODNs to specifically interact with their corresponding TFs by EMSA in conjunction with supershift methods (Fig. 3a) using antibodies directed against NF-κB (p65), E2F, and Stat3 with the nuclear extract from SKBr-3 cells. The binding of NF-κB demonstrated clear supershift. Although the band shift was not seen with E2F and

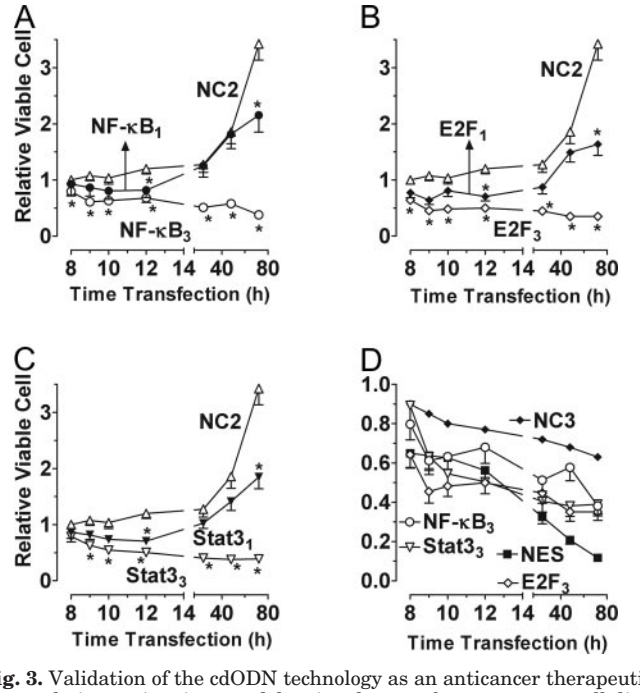

Fig. 3. Validation of the cdODN technology as an anticancer therapeutic approach in an in vitro model using human breast cancer cell line SKBr-3. Time-dependent reduction of cell viability produced by the dODNs: comparisons among the sdODNs, the homogeneous cdODNs, and the heterogeneous cdODN. Data shown were all normalized to the initial values at 0 time point (before ODN transfection). *, $p < 0.05$ versus NC; $n = 6$ independent experiments for each group.

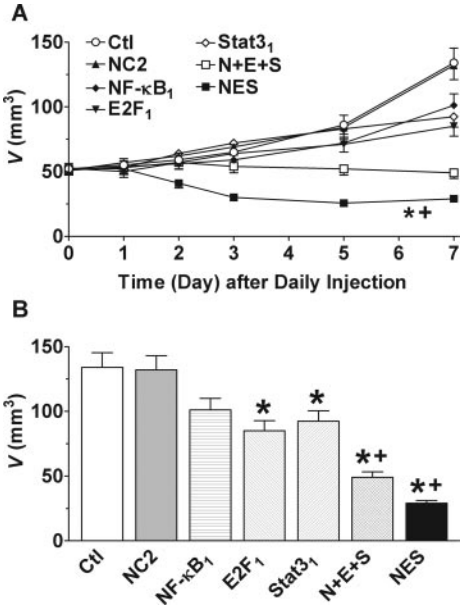

Fig. 4. Validation of the cdODN technology as an anticancer therapeutic approach in an in vivo s.c. model of tumors induced by SKBr-3 cells in nude mice. A, Effects of decoy ODNs on tumor growth as a function time (day) with daily injection of the dODNs. *, $p < 0.05$, *F*-test, NES versus each of the sdODNs: NF-κB_1, $E2F_1$, or $Stat3_1$; +, $p < 0.05$, *F*-test, NES versus N+E+S. B, comparisons of tumor volumes at day 7 after daily dODN injection between the mice treated with the sdODNs (NF-κB_1, $E2F_1$, and $Stat3_1$), coapplication of the sdODNs (N+E+S), and the cdODN (NES). Eight animals were used for each group *, $p < 0.05$ versus NC2; +, $p < 0.05$ versus each of the sdODNs.

Stat3 antibodies, the DNA bands were significantly decreased, indicating the specific bindings of the dODNs with their target proteins. As expected, the cdODNs demonstrated remarkably greater binding with their respective TFs than the sdODNs, as determined by quantification of the bands using ImageQuant software. For example, the band density with NF-κB_3 was 4450 ± 108 pixels, 18 times greater than that with NF-κB_1 (240 ± 18 pixels; likewise, $E2F_3$ was ~12 times greater than $E2F_1$ and $Stat3_3$ was 10 times greater than $Stat3_1$. NES simultaneously binds to all three target TFs (NF-κB, E2F, and Stat3), as indicated by the alternate uses of the antibodies (Fig. 3a).

We then confirmed the efficiency of transfection and the delivery of these cdODNs into the nuclei of cells (Fig. 3b). The accessibility of the cdODNs into their major site of action is clearly indicated by the overlapping (yellow) of dODN (green), and nucleic (red) fluorescence stainings localized to the nuclei. The nucleic staining did not appear until 6 h after transfection, which is consistent with the time course of the cdDNAs on cancer cell growth. The percentage of cells with successful uptake of dODNs was similar between the sdODNs (46%) and the cdODNs (42%), determined by counting cells with clear yellow staining. With time, the percentage of uptake increased. Twenty hours later, the uptake reached 79%, and it took around 18 h to reach the plateau level. To further verify the uptake of cdODN into the cell, we measured the amount of cell-associated NES with FITC-labeled phosphorothioate NES at two different extracellular concentrations ($[NES]_o$ = 100 nM and 1 μM). The data are shown in Fig. 5D, where the intracellular concentration of NES ($[NES]_i$) is plotted as a function of time after transfection. The $[NES]_i$ reached a maximum level within approximately 18 to 24 h and the peak $[NES]_i$ was 8.1 ± 0.7 nM in the presence of 100 nM $[NES]_o$ and 119.5 ± 11.0 nM in the

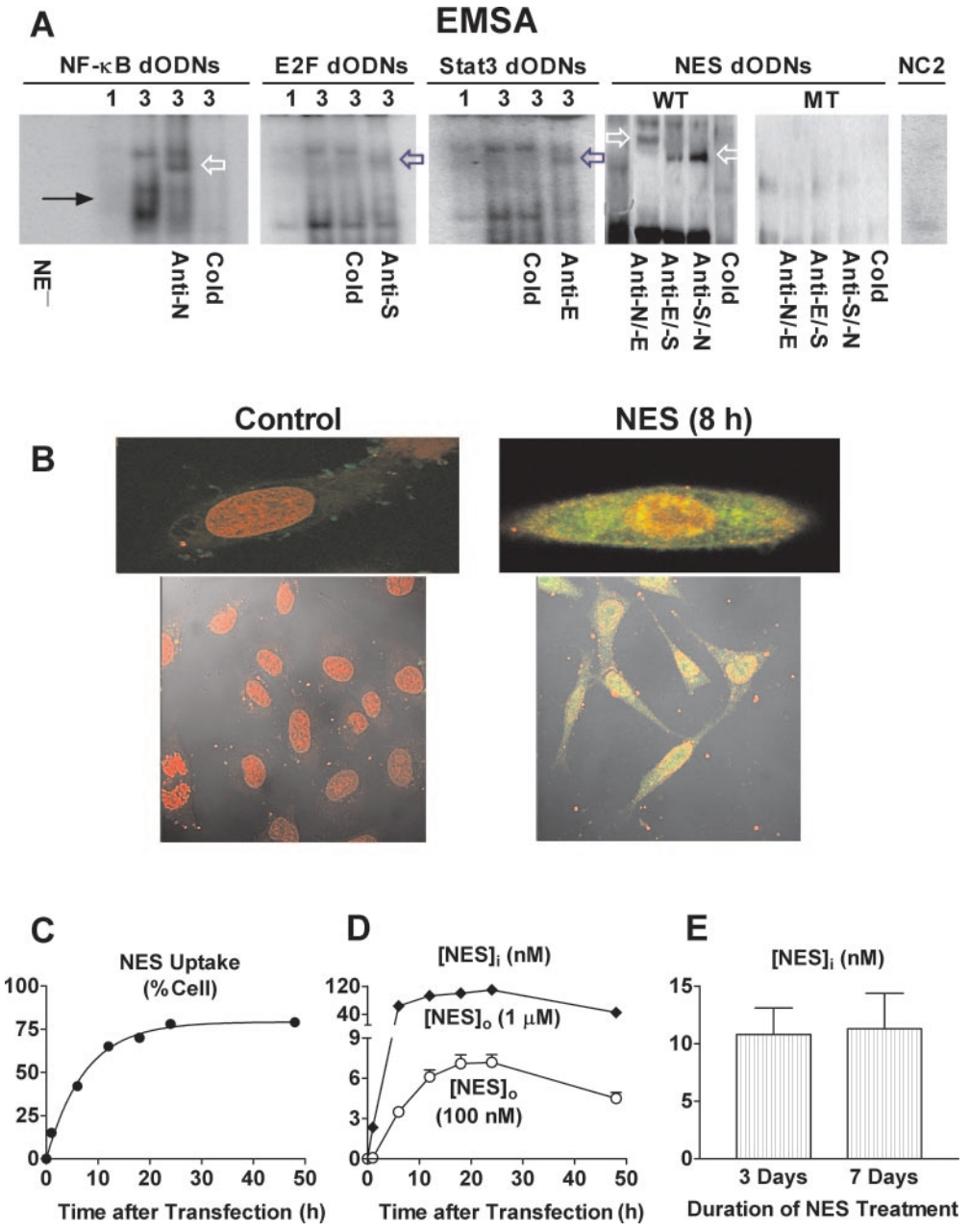

Fig. 5. Validation of dODNs' ability to bind target TFs and to manipulate expression of the target genes. A, EMSA showing the ability of the dODNs to bind the target TFs. The numbers above each lane indicate the number of consensus *cis* elements. The arrows indicate the positions of the DNA-protein complexes. NC2, negative control with a scrambled ODN; NEP^-, nuclear extract minus; Cold, in the presence of unlabeled dODNs; Anti-N (p65), Anti-E, and Anti-S, treated with the antibodies directed against NF-κB, E2F, and Stat3, respectively; and Anti-N/-E, Anti-E/-S, and Anti-S/-N: concomitantly treated with two antibodies, as indicated; WT, wild-type NES; MT, mutant NES (Fig. 1). Arrows indicate the supershift bands. B, subcellular localization of transfected the cdODN (NES). The costaining (yellow) of nuclei with Alexa Fluor 488 (green) and PI (red) indicates the accessibility of the dODNs to the nuclei. Top, magnification, 2000×; bottom, magnification, 100×. C, exponential increase in the percentage of cells (n = 4 batches of cells) with successful uptake of FITC-labeled phosphorothioate NES, determined by flow cytometry. D, quantification of intracellular concentration of FITC-labeled phosphorothioate cdODN ($[NES]_i$) in SKBr-3 cells (n = 3 batches of cells) treated with extracellular concentrations of NES ($[NES]_o$) of 100 nM and 1 μM, respectively, as a function of time after transfection. E, quantification of intracellular concentration of NES ($[NES]_i$) in tumor xenografts in nude mice, 3 and 7 days after daily injections of FITC-labeled phosphorothioate NES into the tumor mass.

presence of 1 μM $[NES]_o$, equivalent to ~8 and ~12% of the 100 nM and 1 μM $[NES]_o$, respectively. The $[NES]_i$ in tumor cells isolated from the xenografts of nude mice was also measured at two time points: 3 and 7 days after daily injection of NES at 100 nM (or $[NES]_o$ = 100 nM). As shown in Fig. 5E, administration of NES to tumor mass for 3 days yielded an $[NES]_i$ 10.8 ± 2.3 nM and for 7 days an $[NES]_i$ 11.3 ± 3.1 nM. The data indicate that daily injection of 100 nM NES created a stable $[NES]_i$, which is comparable with the peak level reached by a single application to SKBr-3 cells.

We subsequently studied the gene interference of the dODNs (100 nM) by quantifying mRNA levels with real-time RT-PCR 18 h after transfection, and the genes studied included Flip (Kreuz et al., 2001; Micheau et al., 2001) and Myc for NF-κB (Duyao et al., 1992; La Rosa et al., 1994); DHFR-(Fry et al., 1999; Park et al., 2003) and CCNE1 (Stanelle et al., 2003; Yasui et al., 2003) for E2F; and p53 (Niu et al., 2005;) and Bcl-2 (Nielsen et al., 1999; Lin et al., 2005b) for Stat3 (Fig. 3c). The dODNs knocked down the transcription of their respective genes. Stat3 dODNs up-regulated p53 transcription, and so did NES. The cdODNs consistently produced more pronounced effects on the transcription than the sdODNs. For example, NF-κB_1 and NF-κB_3 reduced Myc mRNA levels by ~13 and ~48%, respectively. It is also noteworthy that the heterogeneous cdODN NES affected transcription of all the genes examined in this study that are regulated by NF-κB, E2F, and Stat3, respectively (Fig. 6A). It should be noted that overall, the expression of down-regulation in this study is smaller than that in many previous studies using dODNs; this is because the concentration used in this study is lower (100 nM) than in most of the other studies (which generally used >1 μM). Such a concentration might well elicit cytotoxicity in our conditions. To test this notion, we conducted experiments on concentration-dependent down-regulation by NES of three selected target genes: *Myc*, *NNCE1*, and *Bcl-2*. As illustrated in Fig. 6B (left), the extent of expression depression of the target genes was increased with increasing $[NES]_o$. At 10 μM, the gene expression was virtually abolished. For negative controls, concentration dependence of NC2 (scrambled ODN) and NC3 (mutant NES) on expression of the same set of genes was also studied. As shown in Fig. 6B (right), NC2 produced minimal effect on gene expression, and NC3 elicited certain degrees of gene expression inhibition, but the effects did not reach statistical significance ($p > 0.05$).

Discussion

Major Findings of the Study. We show here the superiority of simultaneously targeting multiple oncoproteins over targeting single oncoproteins in inhibiting tumor cell growth under both in vitro and in vivo conditions, in terms of the efficacy, potency, toxicity, and duration of actions. The ability of CpG-containing oligonucleotides to stimulate the innate immune system can yield antitumor efficacy in xenograft tumor models (Sato et al., 1999; Kandimalla et al., 2003). We have analyzed the CpG content of our decoy ODNs and found that none of the dODNs contains the PuPuCGPyPy motif.

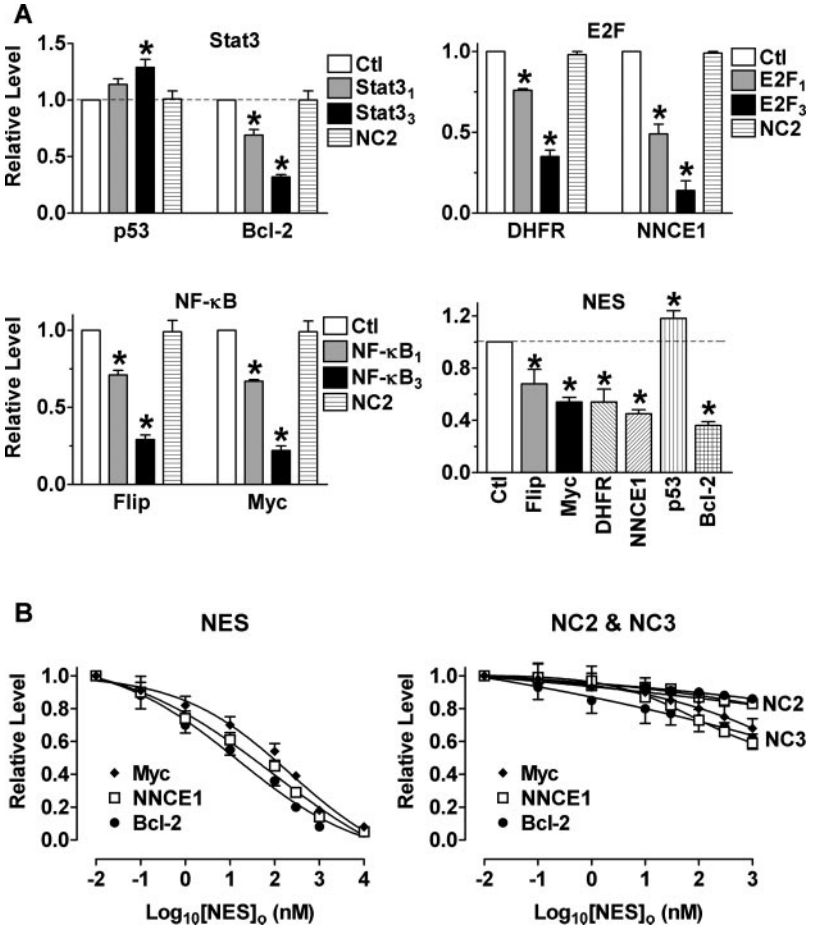

Fig. 6. Validation of dODNs' ability to bind target transcription factors (TFs) and to manipulate gene expression. A, real-time RT-PCR quantification of changes of expression of various genes, produced by dODNs (100 nM). Shown are mean data (n = 5 independent experiments for each group) expressed as relative level of mRNA after normalization to the effects of NC1 or NC2. *, $p < 0.05$ versus NC. B, concentration-dependent down-regulation of the selected genes by NES. Shown are mean data from four independent samples. The data for NES and NC3 were first normalized to those for NC2 and then to the lowest concentration of NES or NC3 (0.01 nM), and NC2 data were not normalized its lowest concentration (0.01 nM). All data are expressed as relative level over control nontreated cells.

Hence, the in vitro effects of the dODNs, both phenotypically and molecularly, are consistent with the in vivo antitumor efficacy; the measurements of biological activity do not strictly correlate with the CpG content of any of the dODNs. The cdODN strategy in this study, besides confirming the specificity, simplicity, and effectiveness of the dODN approach, unravels some novel aspects, and extends the applications of the dODN technology. In addition, the present study also establishes the combination of NF-κB/E2F/Stat3 targeting as a potential anticancer agent worthy of further studies in preclinical settings. The advantages of cdODN are likely to be ascribed to simultaneous interference of expression of multiple genes controlled by the target TFs. The beauty of this cdODN one-drug, multiple-target strategy is that it can be either homogeneous (carrying multiple consensus sites corresponding to a specific TF to enhance the efficacy and potency of desired effects) or heterogeneous (with multiple distinct *cis* elements targeting different TFs).

Potential Implications of the Study. During the past decade, the complete genomes of more than 140 different organisms have been sequenced and made available in databases. These databases provide extremely useful collections of organized, validated data that are indispensable for genomics and proteomics research and the drug discovery process. TFs make up 6% of the human genome, ranking second because of their abundance, and have recently been considered a new class of candidate targets for drug discovery (Roth, 2005). On the other hand, the dODN technology using TFs as molecular targets is emerging as a powerful strategy for gene therapy of a broad range of human diseases (Mann and Dzau, 2000; Morishita et al., 2001). In theory, our cdODN one-drug, multiple-target strategy mimics the well known drug cocktail therapy. Nevertheless, this one-drug, multiple-target strategy is devoid of the weaknesses of the drug cocktail therapy, involving complicated treatment regimens, undesirable drug-drug interactions, and increased side effects. The cdODN strategy offers resourceful combinations of varying *cis* elements for concomitantly targeting multiple molecules, particularly biological processes. In this study, we merely tested the cdODNs potentially applicable to a wide spectrum of cancers, because the target oncoproteins of NF-κB/E2F/Stat3 are not tissue specific. It noteworthy that the cdODN strategy has the potential to target specific types of cancer. For example, a cdODN can be designed to treat breast cancer in particular by targeting SNAIL (a zinc-finger transcription factor) (Martin et al., 2005), the estrogen receptor responsive element (Wang et al., 2003), Brn-3b (Budhram-Mahadeo et al., 1999), SLUG (a zinc-finger transcription factor of the SNAIL family) (Tripathi, 2005), and Ets-binding sites. The estrogen receptor responsive element in the form of decoy has been shown to be effective in suppressing breast cancer cell growth. Brn-3b is a repressor of BRCA1 and SLUG is a repressor of BRCA2 (down-regulation and/or mutations of BRCA1/2 have been shown to be critical for breast cancer development). Moreover, the cdODN strategy can also be applied to other disorders in addition to cancer. For instance, tumor necrosis factor-α, GATA-4, FOG-2, and Janus tyrosine kinase-signal transducer and activator of transcription could be a reasonable combination for a cdODN aiming to treat heart failure by reducing apoptosis (Suzuki and Evans, 2004; Kassiri et al., 2005). A cdODN targeting Irx5, Irx3, and Etv1 may be applied to reduce regional heterogeneity of cardiac repolarization to minimize arrhythmogenesis, because these TFs have been shown to be expressed in transmural gradients across the ventricular wall (Costantini et al., 2006; Rosati et al., 2006) and to be responsible for the transmural difference of a K^+ channel (Costantini et al., 2006). Therefore, the cdODN technology opens the door to one-drug, multiple-target intervention, providing promising prototypes of gene therapeutic agents for a wide range of human diseases.

The cdODN technology also opens up new opportunities for creative and rational designs of a variety of combinations integrating varying *cis* elements for various purposes and provides an exquisite tool for functional genomics analysis related to identification and characterization of new and known transcription factors and their functions in gene controlling program. It can also be used as a simple and straightforward approach for studying any other biological processes involving multiple factors, multiple genes, multiple signaling pathways, etc.

Possible Limitation of the Study. We consider the present work rather preliminary; to completely validate the cdODN technology as a gene therapy strategy, many important issues remain unresolved. The optimal combination of targets for a cdODN remains unknown. In this study, we tested "three-in-one" cdODNs. In theory, "*N*-in-one" cdODNs (N could be any number of *cis*-acting elements) can be designed to include more relevant target TFs; however, larger cdODNs may hinder their penetration into the cells and nuclei and compromise the effectiveness. More rigorous studies are warranted to define the optimal combination of length and accessibility of cdODNs to optimize desired effectiveness. This work does not allow us to draw any conclusions as to what the optimal organization is for multiple *cis* elements to be placed in a single cdODN molecule. Nonetheless, the present study lays the groundwork for future exploitation on these subjects. Efficient delivery of dODNs into a cell is another challenge to using dODNs as therapeutic agents, as in other nucleotide-based technologies such as small interfering RNA, antisense, ribozyme, aptamers, etc. Still another difficulty is to maintain an effective concentration of dODN within a cell for a sufficient period of time. At present, investigation on modifications of dODNs to enhance efficiency of transfection and to strengthen the stability within a cell so as to prolong the duration of actions is an active field of research. Constructing cdODN into virus vectors, such as adenovirus, lentivirus, etc., might be a reasonable choice to at least partially offset the weakness of the nucleotide technologies.

Acknowledgments

We thank XiaoFan Yang for excellent technical support.

References

Ahn JD, Kim CH, Magae J, Kim YH, Kim HJ, Park KK, Hong S, Park KG, Lee IK, and Chang YC (2003) E2F decoy oligodeoxynucleotides effectively inhibit growth of human tumor cells. *Biochem Biophys Res Commun* **310:**1048–1053.

Bielinska A, Shivdasani RA, Zhang L, and Nabel GJ (1990) Regulation of gene expression with double-stranded phosphorothioate oligonucleotides. *Science (Wash DC)* **250:**997–1000.

Budhram-Mahadeo V, Ndisang D, Ward T, Weber BL, and Latchman DS (1999) The Brn-3b POU family transcription factor represses expression of the BRCA-1 anti-oncogene in breast cancer cells. *Oncogene* **18:**6684–6691.

Chan KS, Sano S, Kiguchi K, Anders J, Komazawa N, Takeda J, and DiGiovanni J (2004) Disruption of Stat3 reveals a critical role in both the initiation and the promotion stages of epithelial carcinogenesis. *J Clin Investig* **117:**720–728.

Charpentier G (2002). Oral combination therapy for type 2 diabetes. *Diabetes Metab Res Rev* **18(Suppl 3):**S70–S76.
Costantini DL, Arruda EP, Agarwal P, Kim KH, Zhu Y, Zhu W, Lebel M, Cheng CW, Park CY, Pierce SA, et al. (2006) The homeodomain transcription factor Irx5 establishes the mouse cardiac ventricular repolarization gradient. *Cell* **123:**347–358.
Dolcet X, Llobet D, Pallares J, and Matias-Guiu X (2005) NF-κB in development and progression of human cancer. *Virchows Arch* **446:**475–482.
Duyao MP, Kessler DJ, Spicer DB, Bartholomew C, Cleveland JL, Siekevitz M, and Sonenshein GE (1992) Transactivation of the c-myc promoter by human T cell leukemia virus type 1 tax is mediated by NF kappa B. *J Biol Chem* **267:**16288–16291.
Fry CJ, Pearson A, Malinowski E, Bartley SM, Greenblatt J, and Farnham PJ (1999) Activation of the murine dihydrofolate reductase promoter by E2F1. A requirement for CBP recruitment. *J Biol Chem* **274:**15883–15891.
Henkel J (1999) Attacking AIDS with a 'cocktail' therapy? *FDA Consum* **33:**12–17.
Ji YB, Gao SY, Ji HR, Kong Q, Zhang XJ, and Yang BF (2004) Anti-neoplastic efficacy of Haimiding on gastric carcinoma and its mechanisms. *World J Gastroenterol* **10:**484–490.
Kandimalla ER, Bhagat L, Cong YP, Pandey RK, Yu D, Zhao Q, and Agrawal S (2003) Secondary structures in CpG oligonucleotides affect immunostimulatory activity. *Biochem Biophys Res Commun* **306:**948–953.
Kassiri Z, Oudit GY, Sanchez O, Dawood F, Mohammed FF, Nuttall RK, Edwards DR, Liu PP, Backx PH, and Khokha R (2005) Combination of tumor necrosis factor-alpha ablation and matrix metalloproteinase inhibition prevents heart failure after pressure overload in tissue inhibitor of metalloproteinase-3 knock-out mice. *Circ Res* **97:**380–390.
Konlee M (1998) An evaluation of drug cocktail combinations for their immunological value in preventing/remitting opportunistic infections. *Posit Health News* **16:**2–4.
Kreuz S, Siegmund D, Scheurich P, and Wajant H (2001) NFkappaB inducers upregulate cFLIP, a cycloheximide-sensitive inhibitor of death receptor signaling. *Mol Cell Biol* **21:**3964–3973.
Kumar P (2005) Combination treatment significantly enhances the efficacy of antitumor therapy by preferentially targeting angiogenesis. *Lab Investig* **85:**756–767.
La Rosa FA, Pierce JW, and Sonenshein GE (1994) Differential regulation of the c-myc oncogene promoter by the NF-kappa B rel family of transcription factors. *Mol Cell Biol* **14:**1039–1044.
Leong PL, Andrews GA, Johnson DE, Dyer KF, Xi S, Mai JC, Robbins PD, Gadiparthi S, Burke NA, Watkins SF, et al. (2004) Targeted inhibition of Stat3 with a decoy oligonucleotide abrogates head and neck cancer cell growth. *Proc Natl Acad Sci USA* **100:**4138–4143.
Li C, Zhang F, Lin M, and Liu J (2004) Induction of S100A9 gene expression by cytokine oncostatin M in breast cancer cells through the STAT3 signaling cascade. *Breast Cancer Res Treat* **87:**123–134.
Lin LM, Li BX, Xiao JB, Lin DH, and Yang BF (2005a) Synergistic effect of all-trans-retinoic acid and arsenic trioxide on growth inhibition and apoptosis in human hepatoma, breast cancer, and lung cancer cells in vitro. *World J Gastroenterol* **11:**5633–5637.
Lin Q, Lai R, Chirieac LR, Li C, Thomazy VA, Grammatikakis I, Rassidakis GZ, Zhang W, Fujio Y, Kunisada K, et al. (2005b) Constitutive activation of JAK3/STAT3 in colon carcinoma tumors and cell lines: inhibition of JAK3/STAT3 signaling induces apoptosis and cell cycle arrest of colon carcinoma cells. *Am J Pathol* **167:**969–980.
Lun M, Zhang PL, Siegelmann-Danieli N, Blasick TM, and Brown RE (2005) Intracellular inhibitory effects of Velcade correlate with morphoproteomic expression of phosphorylated-nuclear factor-kappaB and p53 in breast cancer cell lines. *Ann Clin Lab Sci* **35:**15–24.
Mann MJ and Dzau VJ (2000) Therapeutic applications of transcription factor decoy oligonucleotides. *J Clin Investig* **106:**1071–1075.
Mann MJ, Whittemore AD, Donaldson MC, Belkin M, Conte MS, Polak JF, Orav EJ, Ehsan A, Dell'Acqua G, and Dzau VJ (1999) Ex-vivo gene therapy of human vascular bypass grafts with E2F decoy: the PREVENT single-centre, randomized, controlled trial. *Lancet* **354:**1493–1498.
Martin TA, Goyal A, Watkins G, and Jiang WG (2005) Expression of the transcription factors snail, slug, and twist and their clinical significance in human breast cancer. *Ann Surg Oncol* **12:**488–496.
Micheau O, Lens S, Gaide O, Alevizopoulos K, and Tschopp J (2001) NF-kappaB signals induce the expression of c-FLIP. *Mol Cell Biol* **21:**5299–5305.
Morishita R, Aoki M, and Kaneda,Y (2001) Decoy oligodeoxynucleotides as novel cardiovascular drugs for cardiovascular disease. *Ann NY Acad Sci* **947:**294–301.
Morishita R, Gibbons GH, Horiuchi M, Ellison KE, Nakama M, Zhang L, Kaneda Y, Ogihara T, and Dzau VJ (1995) A gene therapy strategy using a transcription factor decoy of the E2F binding site inhibits smooth muscle proliferation in vivo. *Proc Natl Acad Sci USA* **92:**5855–5859.
Morishita R, Sugimoto T, Aoki M, Kida I, Tomita N, Moriguchi A, Maeda K, Sawa Y, Kaneda Y, Higaki J, et al. (1997) In vivo transfection of cis element "decoy" against nuclear factor-kappaB binding site prevents myocardial infarction. *Nat Med* **13:**894–899.
Nabholtz JM and Gligorov J (2005) Docetaxel/trastuzumab combination therapy for the treatment of breast cancer. *Expert Opin Pharmacother* **6:**1555–1564.
Nielsen M, Kaestel CG, Eriksen KW, Woetmann A, Stokkedal T, Kaltoft K, Geisler C, Ropke C, and Odum N (1999) Inhibition of constitutively activated Stat3 correlates with altered Bcl-2/Bax expression and induction of apoptosis in mycosis fungoides tumor cells. *Leukemia* **13:**735–738.
Niu G, Wright KL, Ma Y, Wright GM, Huang M, Irby R, Briggs J, Karras J, Cress WD, Pardoll D, et al. (2005) Role of Stat3 in regulating p53 expression and function. *Mol Cell Biol* **25:**7432–7440.
Ogihara T (2003) The combination therapy of hypertension to prevent cardiovascular events (COPE) trial: rationale and design. *Hypertens Res* **28:**331–338.
Pang L, Koren G, Wang Z, and Nattel S (2003) Tissue-specific expression of two human $Ca_v1.2$ isoforms under the control of distinct 5′ flanking regulatory elements. *FEBS Lett* **546:**349–354.
Park KK, Rue SW, Lee IS, Kim HC, Lee IK, Ahn JD, Kim HS, Yu TS, Kwak JY, Heintz NH, et al. (2003) Modulation of Sp1-dependent transcription by a cis-acting E2F element in DHFR promoter. *Biochem Biophys Res Commun* **306:**239–243.
Roth M (2005) Transcription factors: Are they a real target for future therapeutic strategies? *Pharmacologyonline* **1:**45–66.
Rosati B, Grau F, and McKinnon D (2006) Regional variation in mRNA transcript abundance within the ventricular wall. *J Mol Cell Cardiol* **40:**295–302.
Sato Y, Miyata M, Sato Y, Nishimaki T, Kochi H, and Kasukawa R (1999) CpG motif-containing DNA fragments from sera of patients with systemic lupus erythematosus proliferate mononuclear cells in vitro. *J Rheumatol* **26:**294–301.
Stanelle J, Stiewe T, Rodicker F, Kohler K, Theseling C, and Putzer BM (2003) Mechanism of E2F1-induced apoptosis in primary vascular smooth muscle cells. *Cardiovasc Res* **59:**512–519.
Suzuki YJ and Evans T (2004) Regulation of cardiac myocyte apoptosis by the GATA-4 transcription factor. *Life Sci* **74:**1829–1838.
Tripathi MK (2005) Regulation of BRCA2 gene expression by the SLUG repressor protein in human breast cells. *J Biol Chem* **280:**17163–17171.
Wang H, Zhang Y, Cao L, Han H, Wang J, Yang B, Nattel S, and Wang Z (2002) HERG K^+ channel: A regulator of tumor cell apoptosis and proliferation. *Cancer Res* **62:**4843–4848.
Wang LH, Yang XY, Zhang X, Mihalic K, Xiao W, and Farrar WL (2003) The *cis* decoy against the estrogen response element suppresses breast cancer cells via target disrupting c-fos not mitogen-activated protein kinase activity. *Cancer Res* **63:**2046–2051.
Xi S, Gooding WE, and Grandis JR (2005) In vivo antitumor efficacy of STAT3 blockade using a transcription factor decoy approach: implications for cancer therapy. *Oncogene* **24:**970–979.
Yasui K, Okamoto H, Arii S, and Inazawa J (2003) Association of over-expressed TFDP1 with progression of hepatocellular carcinomas. *J Hum Genet* **48:**609–613.
Yokoyama TH, Nakano H, Yamazaki T, Tamai K, Hanada K, and Takahashi G (2005) Enhancement of ultraviolet-induced apoptosis by NF-kappaB decoy oligonucleotides. *Br J Dermatol* **153 (Suppl 2):**47–51.

Address correspondence to: Dr. Zhiguo Wang, Research Center, Montreal Heart Institute, 5000 Belanger East, Montreal, QC H1T 1C8 Canada. E-mail: wz.email@gmail.com